Available online at www.sciencedirect.com
ScienceDirect
Journal of Nuclear Materials 375 (2008) 144–150
journal of nuclear materials
www.elsevier.com/locate/jnucmat

Simulations of vacancy cluster behavior in δ-Pu

Blas Pedro Uberuaga *, Steven M. Valone

Materials Science and Technology Division, Los Alamos National Laboratory, Los Alamos, NM 87545, USA

Received 30 October 2007; accepted 3 January 2008

Abstract

Using rates for vacancy diffusion in plutonium (Pu) found with parallel-replica dynamics, we develop a kinetic Monte Carlo (KMC) model of void growth and mobility. We compare and contrast the behavior of voids in Pu as predicted using vacancy mobilities from two different modified embedded atom method (MEAM) descriptions of Pu. We find that void behavior depends sensitively on the values used for vacancy mobility. In particular, we find that voids are very mobile in one model of Pu, but are essentially immobile in another, leading to very different void structures over time. This second model also predicts lifetimes for voids that are extremely long, and seemingly unphysical, suggesting that the first model is more representative of real Pu.
Published by Elsevier B.V.

PACS: 61.72.Qq; 61.72.Ji; 07.05.Tp; 21.65.+f

1. Introduction

Plutonium (Pu) is a key component of many important technologies, from the nuclear weapons program to fission reactors. To maximize its potential, maintain safety, and enhance reliability in these applications, its properties must be thoroughly understood. One important property is the structural evolution during self-irradiation, or aging. As Pu atoms decay, the recoils due to the decay create damage in the lattice. This damage, initially consisting of interstitials and vacancies, evolves into larger scale features such as voids and bubbles (when He is present). These larger defects, in turn, govern changes in macroscopic properties such as volumetric expansion and structural stability.

The goal of this work is to examine some evolutionary properties of voids in Pu. We begin by characterizing, using parallel-replica dynamics [1], the mobility of small vacancy defects containing just one or two vacancies using two different parameterizations of Pu within the modified embedded atom method [2,3] description. We then develop a kinetic Monte Carlo model that uses the atomistic results on vacancy diffusion to examine the evolution and mobility of large voids. We find that the predicted behavior of voids depends on which MEAM description we use for Pu. In particular, long-time pore-size distributions differ for the two models. Such results impact continuum level models that track radiation damage evolution [4,5]. Pore-size distribution can affect other properties such as swelling rates, thermal conductivity, and material strength. Finally we observe unexpected transformations of voids into stacking fault tetrahedra (SFTs).

2. Methodology

Our examination of vacancy behavior in Pu relies on two simulation methodologies: parallel-replica dynamics and kinetic Monte Carlo (KMC). Parallel-replica dynamics involves a straight-forward parallelization of time simulated on multiple processors. Each processor evolves an independent replica of the entire system until a transition to a new state is detected on any of the processors. If the rare events that govern dynamics from state-to-state in the material are first order processes, then parallel-replica dynamics is exact, even describing correlated events correctly. Using M processors in parallel, one can reach a

* Corresponding author.
E-mail address: blas@lanl.gov (B.P. Uberuaga).

0022-3115/$ - see front matter Published by Elsevier B.V.
doi:10.1016/j.jnucmat.2008.01.001

maximum speedup compared to standard molecular dynamics (MD) of M times. Reaching this theoretical maximum efficiency depends on how infrequent the events are, as there is some computational overhead involved each time an event is observed. Other details on our use of parallel-replica dynamics as it pertains to studying Pu can be found in Ref. [6]. The events of interest to us are the hoping events associated with vacancy migration and the equilibrium structure of vacancy clusters.

KMC [7], on the other hand, estimates the solution of a set of simultaneously occurring rate processes via a stochastic method. The rates for known mechanisms must be obtained from experimental measurements or, as here, another model or simulation such as parallel-replica MD. The solution method allows for the simulation of much longer times and larger length scales than possible with any type of MD. Given all possible atomic processes and their rates, KMC results in exact dynamics for the system. The disadvantage of this method is that it is typically not possible to know all possible atomic events *a priori*, causing a reduction in the fidelity of the simulation. However, in some cases, even though it is certain that events are missing in the KMC simulation, important insight into the physical system can still be obtained.

3. Plutonium

Pu is an extremely complicated material, exhibiting more allotropes at ambient pressure (6) than any other element. Correctly describing this behavior theoretically has proven challenging, and even the best density functional theory methods have problems accurately describing the δ-phase. In the following work, we use the modified embedded atom method (MEAM) [2,3] to describe the Pu–Pu interaction. This potential is remarkable in that it correctly predicts the relative volume changes of each of the six allotropes of Pu.

We have discussed the particulars of applying parallel-replica dynamics to this system before [6]. Here, we note that the simulations are performed under constant volume conditions and that the temperature of some of the parallel-replica simulations are higher than the melting temperature of Pu (about 913 K). For more details about the simulations, the reader is referred to Ref. [6].

4. Mono- and di-vacancy diffusion in Pu

Past experimental work has yielded a consistent picture of self-diffusion in δ-Pu via vacancies that included tracer diffusion and creep experiments (see Ref. [8] and references therein). As summarized by Fluss et al. [9], the measured activation energy for the vacancy component of self-diffusion is 1.3 ± 0.3 eV. This activation energy is the sum of the vacancy formation energy and the energy barrier for vacancy migration. KMC simulations, in an effort to reproduce experimental results, find the migration energy of vacancies to be about 0.55 eV [9]. However, earlier experiments found a slightly higher value for the migration energy of 1.1 ± 0.3 eV [10].

Table 1
Prefactor and migration barrier for vacancy mobility in Pu as calculated using the Pu_4 and Pu_X parameterizations of MEAM

	Mono-vacancy		Di-vacancy	
	ν_{mono} (s^{-1})	E_{mono} (eV)	ν_{di} (s^{-1})	E_{di} (eV)
Pu_4	5.0×10^{12}	1.06	6.4×10^{13}	*1.00*
Pu_X	5.3×10^{13}	1.06	2.4×10^{12}	*0.48*

The principle difference between the two is in the migration barrier for di-vacancy diffusion.

We have calculated mono- and di-vacancy diffusion in Pu for two different parameterizations of MEAM using parallel-replica dynamics. These two parameterizations are referred to here as Pu_4 and Pu_X. The parameterizations for these two models can be found in Ref. [11] and [12], respectively. In summary, the difference between the two parameterizations is a small change in phase stability between δ and α. Pu_4 has the α-phase more stable relative to δ than Pu_X. This is accomplished in two ways. One is by altering the parameter that controls whether inversion symmetry in the local crystal structure increases or decreases the cohesive energy relative to the δ-phase, and by how much. The other has to do with the mechanism of 'screening' whereby the pair interactions are smoothly transitioned between 1st and 2nd nearest neighbors values.

Vacancy mobilities predicted by Pu_4 have been described elsewhere [6]. We performed a similar study for vacancy behavior in Pu_X. The vacancy mobilities in Pu_X are compared with those found in Pu_4 in Table 1.

The main difference between the mobilities of vacancies predicted by Pu_4 and Pu_X is in the migration barrier of the di-vacancy. The migration barrier for the mono-vacancy is essentially identical in both descriptions. While the rate prefactors for both the mono- and di-vacancy differ in each description by an order of magnitude (with Pu_4 predicting a smaller prefactor for mono-vacancy diffusion and a larger one for di-vacancy diffusion compared to Pu_X), these are relatively small differences, dwarfed, at most temperatures, by the difference in the di-vacancy migration barrier. Pu_X predicts a di-vacancy migration barrier that is about half of that predicted from Pu_4. This means that, even taking into account the higher rate prefactor predicted by Pu_4, the rate of di-vacancy diffusion is predicted by Pu_X to be 10^4 times greater at $T = 500$ K than as predicted by Pu_4. Thus, the evolution of vacancies and vacancy clusters predicted by the two models will be very different.

5. KMC model of vacancy clusters

In order to understand the consequences of the difference in di-vacancy mobility on void behavior, we have constructed a simple KMC model that incorporates the atomic-scale mobilities found via parallel-replica dynamics. The model has two components: the stability of vacancy

clusters and the mobility of vacancies in the presence of other vacancies.

We have calculated the binding energy of voids as a function of the number of vacancies n contained within the void. Pu, as predicted by MEAM, is a distorted FCC structure. As a result, there are many local minima around any atomic structure that makes defining the energy of the structure somewhat vague. In calculating binding energies, we have started with a compact vacancy arrangement, forged by removing a central atom and the $(n-1)$ atoms surrounding it to create a void of n vacancies. We then used molecular dynamics (MD) to explore the distortions around that initial structure. Each MD simulation was done at 400 K for a total time of 500 ps. We minimized the structure at regular time intervals (every 5 ps) to determine the lowest energy distortion E_{void} for that vacancy configuration. Using E_{void}, we defined the binding energy of the vacancy cluster as $E_{\text{bind}} = (E_{\text{void}} + (n-1)E_{\text{perfect}}) - nE_{\text{mono-vac}}$ where E_{perfect} is the energy of defect-free FCC Pu and $E_{\text{mono-vac}}$ is the energy of one vacancy in Pu. The results for both Pu_4 and Pu_X are shown in Fig. 1 where the binding energy is scaled by the number n_b of 'bonds' between vacancies in the void. This scaled binding energy is $\epsilon_{\text{bind}} = E_{\text{bind}}/n_b$. There are two main conclusions from Fig. 1: (1) except for the di-vacancy ($n_b = 1$), the binding energy measured as a function of n_b is relatively constant and (2) clusters in the Pu_4 model are more tightly bound than in the Pu_X model. As ϵ_{bind} is relatively constant for larger sizes, in the KMC model we assume all bonds contribute equally in determining the energy of a vacancy cluster and use -0.15 eV/bond for Pu_4 and -0.08 eV/bond for Pu_X.

The second component of the KMC model is the mobility of vacancies. The main difference in vacancy mobility between Pu_4 and Pu_X is that the di-vacancy is much more mobile in Pu_X than in Pu_4. This is because, in Pu_X, the di-vacancy is able to take advantage of the extra room associated with the two missing atoms: when the di-vacancy diffuses, the migrating atom moves into the space created by the second vacancy in the pair. This does not happen to nearly as great an extent in Pu_4. We have performed parallel-replica simulations on vacancy clusters larger than $n = 2$ and found that, while the diffusive behavior is more complicated than for the smaller species (a fact we will comment on later), larger clusters 'diffuse' in a way reminiscent of the di-vacancy. That is, only one atom tends to move during each event and it does so by moving into the empty space created by the other vacancies composing the cluster. We have not been able to fully characterize the diffusive behavior of these clusters, as the large number of local minima associated with the distortions described above both make the parallel-replica simulations less efficient as well as render analyzing the motion more difficult. However, the rate of individual vacancy hops associated with these clusters appears to be closer to that of the di-vacancy than the mono-vacancy. Thus, we assume that there are two diffusive modes for vacancies in Pu: one for mono-vacancies and one for all other vacancy clusters, with a hop rate related to the di-vacancy hop rate. These two basic rates are defined as $k_{\text{mono}} = \nu_{\text{mono}} \exp(-E_{\text{mono}}/k_B T)$ and $k_{\text{di}} = \nu_{\text{di}} \exp(-E_{\text{di}}/k_B T)$.

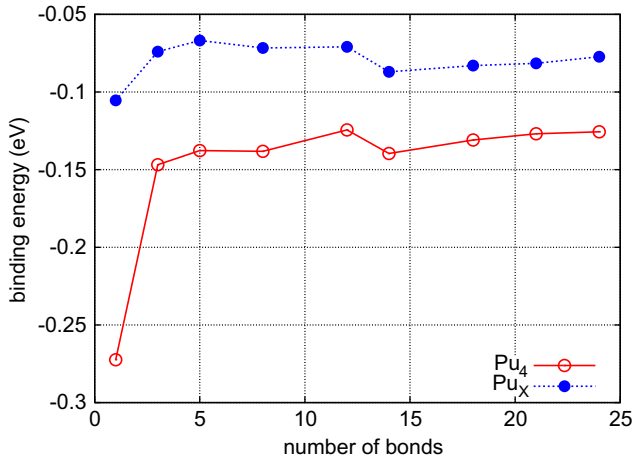

Fig. 1. Binding energies of vacancies in voids in Pu as a function of void size, measured per 'bond' in the void, for both Pu_4 and Pu_X.

The two components above then define our KMC simulation. We define the vacancy configuration on a FCC lattice; there are no off-lattice structures. For each vacancy i, we calculate the number of nearest neighbor vacancies n_i it has. For all possible moves the vacancy can execute (to all neighboring, unoccupied lattice positions j), we calculate the number of neighboring vacancies it would have in the new configuration n_j, giving the change in the number of bonds $\Delta n_{ji} = n_j - n_i$. This defines, via the binding energy per bond ϵ_{bind}, the change in binding energy between the initial and potentially final configuration. If $n_i = 0$, the vacancy has no neighbors in its initial state and the rate to hop to any adjacent site is just k_{mono}. If $n_i > 0$ and $\Delta n_{ji} \geqslant 0$, then we assume that motion for that vacancy is diffusion limited: the new cluster would have a binding energy greater than the initial cluster and the vacancy just has to overcome the migration barrier to access the new state. Furthermore, the vacancy has at least one neighboring vacancy in its initial state so it will hop with a rate of k_{di}. Finally, if $\Delta n_{ji} < 0$, the new state is less stable than the original state and the vacancy has to break one or more bonds to execute the move; the effective barrier is the di-vacancy migration barrier plus the energy of the bonds that are broken. This leads to three conditions

$$n_i = 0; \quad k_{ij} = k_{\text{mono}}, \tag{1}$$

$$n_i > 0 \text{ and } \Delta n_{ji} \geqslant 0; \quad k_{ij} = k_{\text{di}}, \tag{2}$$

$$n_i > 0 \text{ and } \Delta n_{ji} < 0; \quad k_{ij} = k_{\text{di}} \exp(e_{\text{bind}} \Delta n_{ji}/k_B T), \tag{3}$$

where k_{ij} is the rate to hop from position i to position j. In the standard KMC way [7], the rate for each vacancy to hop to each empty neighbor site is calculated and one is selected at random according to its relative weight. The clock is then advanced by the appropriate time. Thus, the dynamical evolution of the system can be monitored.

It should be noted that a number of physical effects are missing from this model. First, no long-range elastic effects are included. Thus, there are no strain-mediated interactions between clusters. Also, as this particular KMC model is lattice-based, off-lattice structures are not allowed. We have seen that off-lattice structures, such as stacking fault tetrahedra, can be very important in describing the evolution of vacancy clusters in FCC metals [13]. However, even small amounts of He stabilize void structures, and He is always present in Pu, so this approximation is reasonable. Second, the mobility of vacancies is described solely as either of mono- or di-vacancy type; if larger clusters have unique diffusive characteristics, that is not considered here. Furthermore, only single vacancy hops are accounted for. We have seen that double hops can occur in Pu [6]. For simplicity, however, we neglect those here. Third, the structure of vacancy clusters is determined solely by the binding energy, as defined by extrapolation from small clusters. These, in turn, were not optimized versus vacancy structure, but rather just against lattice distortion. If larger clusters prefer a non-spherical shape, that is neglected. Finally, there are no thermal expansion effects in this model, corresponding to constant volume conditions.

However, despite these short-comings of the model, we expect that this KMC model will reveal essential differences between vacancy cluster evolution as predicted by Pu_4 versus Pu_X. This will give qualitative predictions that might be examined by experiment to validate one model versus the other, for example by the presence or absence of a particular void size distribution.

6. Void evolution and mobility

We performed KMC simulations under a number of equivalent conditions for both Pu_4 and Pu_X. These conditions do not necessarily mimic any real experimental situation, but rather elucidate the differences between the two models.

6.1. Void stability

First, we examined the lifetime of vacancy clusters as a function of size n and temperature for both models. The results are shown in Fig. 2. The lifetime is measured as the time required for a void initially containing n vacancies to decompose entirely into mono- and di-vacancies. KMC simulations were allowed to run until either the simulation time reached 3×10^{10} s or 10^8 KMC steps were taken. If either of these conditions were reached, it is assumed that the void is stable and no lifetime is assigned. In reality, some of the voids partially decomposed within these limits, but in most cases, only a few vacancies had been released before the simulation ended.

There are three main conclusions to be reached from Fig. 2. First, as would be expected, the lifetime depends on void size n, with larger voids taking longer times to decompose. Second, for both Pu_4 and Pu_X, voids of size

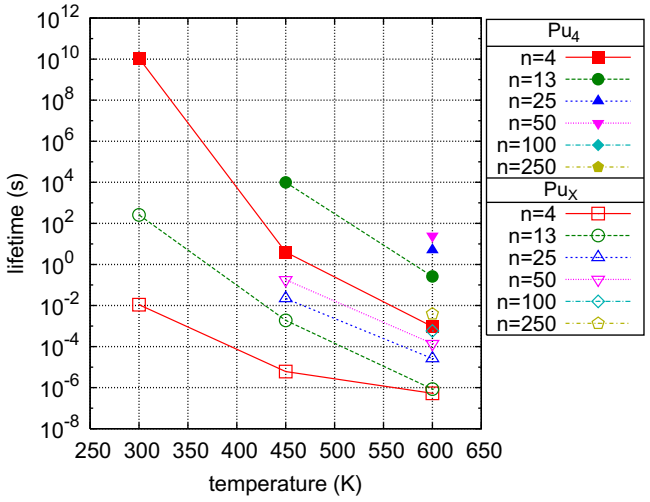

Fig. 2. Lifetime of voids as a function of initial void size for both Pu_4 (filled symbols) and Pu_X (open symbols).

$n = 100$ and larger are relatively stable for temperatures below 600 K. Such voids do not decompose to mono- and di-vacancies within the simulation limits specified above. Finally, because of the weaker binding energies and higher mobilities associated with the Pu_X model, voids are predicted to decompose much faster compared to Pu_4. At room temperature, these differences can be extremely large; for $n = 4$, the lifetimes differ by a factor of 10^{12}. These differences would clearly have consequences in predictions of aging properties of Pu. A homologous Stage V annealing temperature of 0.5, where vacancy clusters begin to dissolve and all defects are expected to be mobile, is approximately 460 K, based on the Pu melting point of 920 K. In the Pu_4 model, vacancy clusters larger than 13 vacancies do not dissolve within about 1000 years at temperatures of about 450 K. This suggests that the Pu_X model is more physically reasonable.

6.2. Void formation

Next, we examined the process of void formation. In this case, we started with 100 mono-vacancies in a simulation cell 11.6^3 nm^3. This corresponds to a vacancy concentration of about 3%. Keeping the concentration fixed, we evolved the system forward in time, allowing the mono-vacancies to coalesce into voids. Fig. 3 compares the time to form voids in Pu_4 versus Pu_X at $T = 300$ K. Simulations were run until the system reached a near steady-state condition or the size of the largest clusters remained constant for some time. It is clear that voids form more quickly in Pu_X compared to Pu_4. In fact, the Pu_X system reached a near steady-state condition before the Pu_4 system performs even a single vacancy hop. This is expected as vacancy mobilities are higher in Pu_X and thus vacancies can find one another faster in that model. Fig. 3 also shows that, in Pu_4, the mono-vacancy concentration quickly drops to zero while the size of the largest void is smaller than in

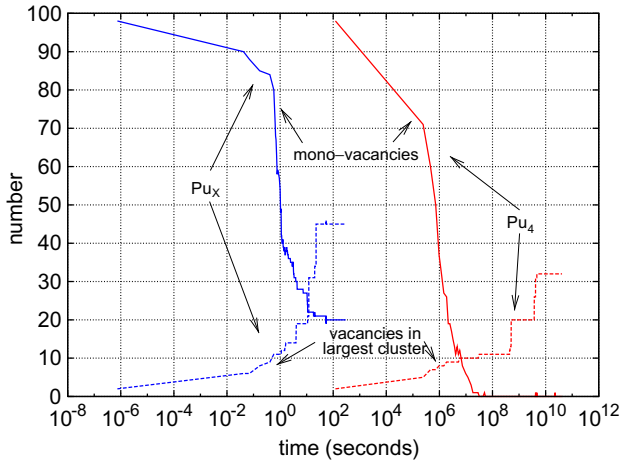

Fig. 3. Comparison of the time to form voids in Pu_4 versus Pu_X at 300 K, starting with 100 mono-vacancies. The number of mono-vacancies remaining in the system as a function of time is shown by the solid lines while the dashed lines show the size of the largest void.

Pu_X. In contrast, in Pu_X, the concentration of mono-vacancies initially falls very quickly but then decays much more slowly as larger voids are formed. This is a result of the differing mobilities of di-vacancies in Pu_4 versus Pu_X. In our KMC model, surface diffusion of vacancies on the void surface occurs with the diffusion rate of di-vacancies in the bulk, modified by the relative binding energy between the initial and final vacancy position. In Pu_X, di-vacancies are much more mobile than mono-vacancies. This means that vacancy mobility on void surfaces is much higher than it is for mono-vacancies. In contrast, in Pu_4, di-vacancies and mono-vacancies diffuse with similar rates. Thus, in Pu_4, voids grow by mono-vacancies encountering existing voids. In Pu_X, however, voids grow by the voids diffusing to find mono-vacancies. This explains the residual mono-vacancy concentration in the Pu_X simulation – the voids have not yet found all of the mono-vacancies. The two models predict, then, very different routes for void evolution in Pu. Fig. 4 shows the difference in vacancy distributions in the two models at $T = 300$ K after 1.25×10^7 KMC steps (resulting in simulation times of 3.8×10^{10} s for Pu_4 and 2.7×10^2 s for Pu_X).

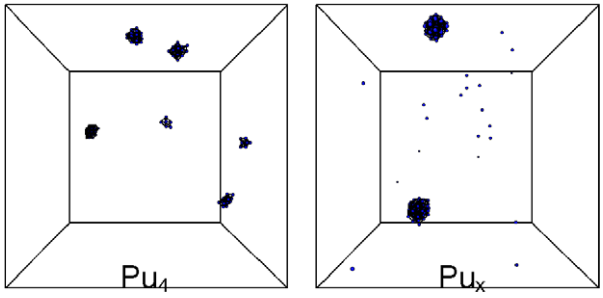

Fig. 4. Comparison of the structure of voids in Pu_4 versus Pu_X at 300 K after the annealing of 100 mono-vacancies at 300 K for 3.8×10^{10} s for Pu_4 and 2.7×10^2 s for Pu_X. The Pu_4 system only forms a couple of small clusters in a time of 2.7×10^2 s.

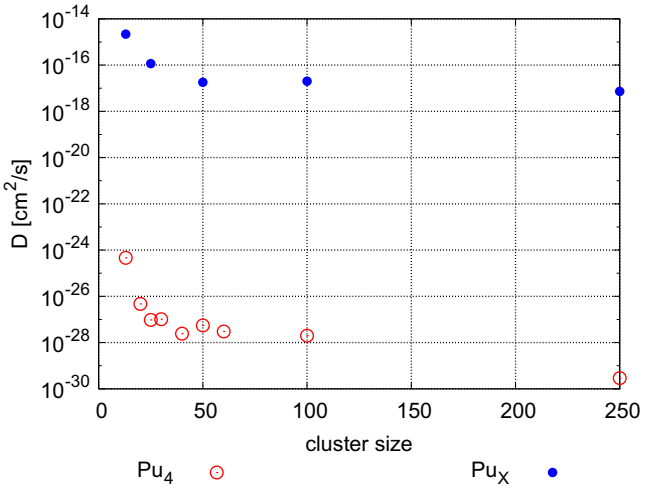

Fig. 5. Comparison of the mobility of the center-of-mass of voids in Pu_4 versus Pu_X at 300 K as a function of void size.

6.3. Void mobility

Finally, we calculated the mobility of voids as a function of void size for both models at 300 K. We calculated the diffusivity of a given void from the mean squared displacement (MSD) of the center-of-mass of the void via

$$\mathrm{MSD} = \frac{1}{N}\sum_{j=1}^{N}(\mathbf{r}_j - \mathbf{r}_{j-1})^2, \tag{4}$$

where each section of the trajectory j corresponds to a given length of time Δt and $\mathbf{r}$ is the center-of-mass position at the corresponding time. In order to ensure that our results were converged, we increased Δt until the MSD attained a constant slope with time. Simulations were performed until either the void size reduced from the initial size or 2×10^8 KMC steps were completed. The results are shown in Fig. 5. While there is some scatter in the results, due primarily to the difficulty in obtaining converged statistics from the KMC simulation, the trends are clear. For both models, void mobility is reduced as void size increases. For Pu_X, the mobility of voids containing 250 vacancies is about 300 times slower than voids containing only 13 vacancies. In Pu_4, the difference in mobility is even greater: 13-vacancy voids are 1.7×10^5 more mobile than voids with 250 vacancies. Furthermore, the enhanced diffusion of di-vacancies in the Pu_X model results in enhanced mobility of voids as well. Voids in Pu_X are between 4.8×10^9 and 2.5×10^{12} times more mobile than in Pu_4, with even greater mobility for larger voids. For comparison, di-vacancy mobility at 300 K is about 2×10^7 greater in Pu_X than Pu_4.

7. Discussion and conclusions

These results clearly show that the behavior of complex defects in Pu is very sensitive to the fundamental point

defect properties underlying those more complex defects. Point defect properties, in turn, depend on the underlying potential. By modifying the potential only slightly, completely different behavior is predicted for the di-vacancy which leads to vastly different predictions for void formation and mobility. The modification from Pu_4 to Pu_X primarily concerns the relative stability of the α and δ-phases of the metal. In fact, the modification was made to produce a model with better Ga stabilization characteristics. Here, of course, we are focused exclusively on the pure Pu metal, and are relying on the constant volume boundary conditions of our simulation cells to mimic the Ga stabilization.

The underlying assumption we have made about a collection of vacancies is that spherical voids are their most stable arrangement. However, as we have recently shown [13], there is a strong entropic driving force for voids to transform to stacking fault tetrahedra (SFTs). In that work, we demonstrated the mechanism for Cu. We have seen a similar mechanism occurring in Pu as well, which is even more surprising as the energy of a SFT compared to a void is significantly higher. Fig. 6 shows the energy profile of a 20-vacancy void as it transforms to a SFT found via a parallel-replica dynamics simulation at 550 K. The mechanism here appears to be very complex, with the transformation being preceded by the apparent break-up of the void (see middle image of Fig. 6). The final SFT is between 2 and 2.5 eV higher in potential energy than the original void; as in the case of Cu, this is an entropically-driven transformation. As shown in Ref. [13], the effective volume of Pu before and after the void-to-SFT transformation can be regarded as having increased by the volume of the void. The relationship for the entropy change ΔS accompanying this volume change ΔV is approximately $\Delta S = \alpha B \Delta V$, where α is the coefficient of volumetric thermal expansion and B is the bulk modulus. For Cu, this gives increases in entropy that agree well with the observed values [13].

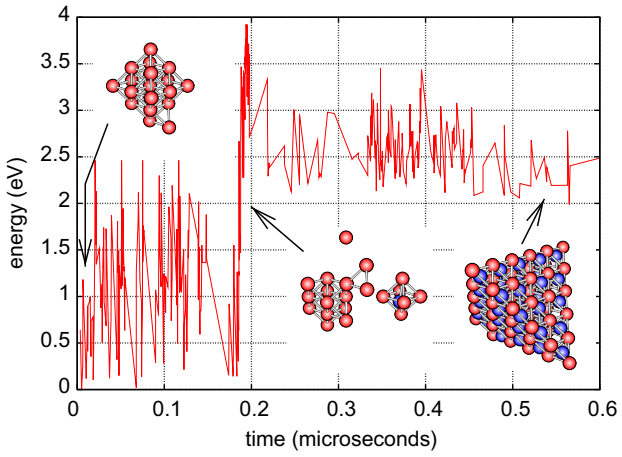

Fig. 6. Transformation of a 20-vacancy void to a stacking fault tetrahedron in the Pu_X model of Pu at $T = 550$ K.

This result would suggest that, indeed, spherical voids are not the preferred arrangement for vacancy clusters in Pu. However, during nuclear fission and Pu metal aging, there will be ample He in the crystal and these He will stabilize void structures. It is well known that even small amount of He stabilize void structures in FCC metals (see, e.g., Refs. [14–17] and references therein). We have seen in simulations in Cu that even one He present in a 20-vacancy void significantly retards the transformation rate. At the higher He loadings typical of Pu, we do not expect that this transformation mechanism will occur at any significant rate. Thus, while this void-to-SFT transformation mechanism is certainly intriguing, its possible role in real Pu is unclear. However, for completeness, we note that small vacancy clusters of size 3–10 that have undergone a similar transformation are mobile in their SFT-like state.

There is not much experimental data that can be directly compared to our results. As discussed by Fluss et al. [9], previous experimental data put the activation energy for self-diffusion via vacancies at 1.3 ± 0.3 eV [8]. If one assumes the typical FCC behavior that 60% of the activation energy is due to vacancy formation and the remaining 40% is due to vacancy migration, the vacancy migration energy in δ-Pu would be between 0.4 and 0.6 eV. Such a value is supported by KMC simulations fit to reproduce experimental observations. A recent study by Timofeeva [10] found a value of 1.1 ± 0.3 eV. The Timofeeva study was on Ga-stabilized δ-Pu and the higher value for the vacancy migration energy might be the result of vacancy interaction with Ga. The value we find for the migration energy of the di-vacancy in the Pu_X model, 0.48 eV, agrees well with the estimated value between 0.4 and 0.6 eV. However, the migration energies we find for the mono-vacancy in both models and the di-vacancy in Pu_4, about 1 eV, agree with the Timofeeva work. Thus, at this time, it is unclear which model is more physically realistic.

Finally, it is interesting to note that recent work on surface diffusion and growth has shown that the size distribution of islands on surfaces depends on the mobility of smaller adatom clusters [18]. In that work, it was found that if only adatoms are mobile, the size distribution of islands is wider than if larger adatom clusters are also mobile. That is, the island size distribution is narrower if larger units are mobile. Similarly, in Pu, our results would suggest that the size distribution of void sizes in Pu_X would be narrower than in Pu_4. This may be one aspect for comparison with experimental observations that could be used to discriminate between the Pu_4 and Pu_X models.

To conclude, using a combination of parallel-replica dynamics and kinetic Monte Carlo (KMC), we have examined the behavior of vacancies and their aggregates as described by two different parameterizations of the modified embedded atom method for Pu. We find that the two models differ most significantly in their prediction of the mobility of the di-vacancy, with the Pu_X model predicting a much higher mobility than the Pu_4 model. This difference

has a profound impact on the structural and pore-size distribution properties of vacancy clusters, as described in a simplified KMC model of the system. While voids have a much longer lifetime in the Pu_4 model, they are much more mobile in the Pu_X model. This tends to result in fewer larger voids in Pu_X and more smaller voids in Pu_4 after vacancy aggregation.

Acknowledgements

We would like to acknowledge helpful discussions with A.F. Voter and M.I. Baskes. This work was funded by the DOE Enhanced Surveillance Campaign. Los Alamos National Laboratory is operated by Los Alamos National Security, LLC, for the National Nuclear Security Administration of the US DOE under Contract DE-AC52-06NA25396.

References

[1] A.F. Voter, Phys. Rev. B 57 (1998) R13985.
[2] M.I. Baskes, J.S. Nelson, A.F. Wright, Phys. Rev. B 40 (1989) 6085.
[3] M.I. Baskes, Phys. Rev. B 46 (1992) 2727.
[4] C.M. Schaldach, W.G. Wolfer, in: M.L. Grossbeck, T.R. Allen, R.G. Lott, A.S. Kumar (Eds.), The Effects of Radiation on Materials, ASTM STP 1447, ASTM International, West Conshohocken, PA, 2003.
[5] H. Trinkaus, B.N. Singh, S.I. Golubov, J. Nucl. Mater. 283–287 (2000) 89.
[6] B.P. Uberuaga, S.M. Valone, M.I. Baskes, J. Alloy Compd. 444–445 (2007) 314.
[7] A.F. Voter, in: K.E. Sickafus, E.A. Kotomin, B.P. Uberuaga (Eds.), Radiation Effects in Solids, Springer, NATO Publishing Unit, Dordrecht, Netherlands, 2006, p. 1.
[8] W.Z. Wade, J. Nucl. Mater. 38 (1971) 292.
[9] M.J. Fluss et al., J. Alloy Compd. 368 (2004) 62.
[10] L.F. Timofeeva, in: K.K.S. Pillay, K.C. Kim (Eds.), International Conference on Plutonium-Future – The Science: Topical Conference on Plutonium and Actinides, AIP Conference Transactions, 2000, p. 11.
[11] M.I. Baskes, Phys. Rev. B 62 (2000) 15532.
[12] M.I. Baskes, A.C. Lawson, S.M. Valone, Phys. Rev. B 72 (2005) 014129.
[13] B.P. Uberuaga, R.G. Hoagland, A.F. Voter, S.M. Valone, Phys. Rev. Lett. 99 (2007) 135501.
[14] K. Farrell, Rad. Eff. 53 (1980) 175.
[15] L.D. Glowinski, J. Nucl. Mater. 61 (1976) 8.
[16] S.K. McLaurin, R.A. Dodd, G.L. Kulcinski, J. Nucl. Mater. 117 (1983) 208.
[17] S.J. Zinkle, W.G. Wolfer, G.L. Kulcinski, L.E. Seitzman, Philos. Mag. A 55 (1987) 127.
[18] M. Basham, F. Montalenti, P.A. Mulheran, Phys. Rev. B 73 (2006) 045422.